Physicochemical Characterization of High- and Low-Melting Phenylephrine Oxazolidines

Yihong Qiu,[1,2] Ronald D. Schoenwald,[1] and J. Keith Guillory[1,3]

Received August 3, 1993; accepted March 26, 1993

Phenylephrine oxazolidine is a new prodrug of phenylephrine developed for improving ocular absorption and reducing systemic side effects. In the present study, high- and low-melting phenylephrine oxazolidines (HMP and LMP) were characterized in terms of their stereochemistry and crystal properties. It was found that the molecular configuration of the prodrug in the crystals of either HMP or LMP is identical (5R/2R). The two crystals were shown to have the same IR spectra and X-ray diffraction patterns but different crystal habits, thermal properties, solubilities and intrinsic dissolution rates. Single crystal X-ray structure analysis indicates that crystals of both HMP and LMP are orthorhombic and belong to the $P2_12_12_1$ space group with four molecules in a unit cell (a = 20.697 Å, b = 7.065 Å, and c = 9.304 Å). The molecules in the crystal are held together by an intermolecular hydrogen bonding interaction between N(3) and O(13). The different physical properties observed for LMP result from crystal imperfections caused by the presence of trace amounts (often at levels <0.5%) of an unidentified, structurally related synthetic impurity which can be dispersed in the prodrug. It was observed that both HMP and LMP can sustain thermal and mechanical treatment in the solid state. However, LMP was partially converted to HMP when suspended in certain solvents.

KEY WORDS: phenylephrine oxazolidine; stereochemistry; intrinsic dissolution; thermal microscopy; scanning electron microscopy; powder X-ray diffractometry; single crystal X-ray diffraction; crystal imperfections.

INTRODUCTION

Phenylephrine oxazolidine (PO) is a lipophilic prodrug of phenylephrine (Fig. 1) which was developed for rapid penetration through the cornea. In rabbits, monkeys, and human volunteers, topical administration of 1% PO produced approximately equal mydriasis compared to 10% phenylephrine hydrochloride (PE), which substantially reduced the potential for cardiovascular effects (1–4). During the development of the product, preformulation studies showed that there were two melting-point forms of PO in the purified synthetic product, each with different physical properties.

Although polymorphism is a relatively common occurrence and, therefore, a likely explanation for the existence of the two forms, diastereoisomers were also a possibility since during chemical synthesis the condensation reaction between *l*-phenylephrine and pivalaldehyde introduced a second asymmetric carbon at C2 with retention of the stereochemical configuration at C5. Crystal imperfections introduced by the presence of trace amounts of a structurally related synthetic impurity (often less than 0.5%) have also been shown to affect crystal habit, thermal properties, specific surface area, and dissolution rate. Therefore, the high- and low-melting phenylephrine oxazolidines (HMP and LMP) could be a result of polymorphism, diastereoisomerism, and/or crystal imperfections, any of which could have important pharmaceutical implications.

The objectives of this study were to determine whether high- and low-melting oxazolidines (HMP and LMP) have the same stereochemistry and to characterize the physical behavior of the crystalline solids.

MATERIALS AND METHODS

Reagents and Chemicals

High- and low-melting phenylephrine oxazolidines were obtained from Sterling Organics (Control Nos. 339-172B and 339-172C, Rensselaer, NY). All reagents used were either HPLC grade or analytical reagent grade.

Characterization of Crystals

Hot Stage Microscopy. Samples which consisted of a few crystals were viewed through a microscope (Bausch & Lomb, Buffalo, NY) at low (10×) power as they were heated at 5°C/min on a hot stage (FP-82, Mettler Instrument Corp., Hightstown, NJ) controlled by a central processor (FP-80, Mettler Instrument Corp.).

Differential Scanning Calorimetry. Experiments were conducted in which the heat of fusion (ΔH_f), melting point, and purity were determined using a differential scanning calorimeter (DSC-7, TAC 7/7 Instrument Controller and 7700 Professional Computer, Perkin-Elmer Corp., Norwalk, CT). The calorimeter was operated at a heating rate of 1.0°C/min and a nitrogen purge was maintained throughout each run. The system was calibrated for temperature and heat of fusion using ultrapure indium (m.p. = 156.6°C, ΔH_f = 28.45 J/g).

Infrared Spectroscopy. Six milligrams of the sample was combined with 294 mg of finely ground potassium chloride and agitated in a cylindrical agate mortar for 20 sec using a mechanical mixer (Wig-L-Bug, Crescent Dental Mfg. Co., Lyons, IL). Diffuse reflectance FT-IR spectra obtained over a wave-number range of 2000 to 400 cm^{-1} were the result of 300 coadded interferograms. Spectra of solid samples were obtained as potassium bromide pellets on a Fourier-transform infrared spectrophotometer (Model 5DXB, Nicolet Instrument Corp., Madison, WI) equipped with a deuterated triglycine sulfate (DTGS) detector, a plotter and data station, and operated under a dry air purge. Spectra were recorded over a wave-number range of 4000 to 400 cm^{-1} on the same instrument.

X-Ray Powder Diffraction. X-ray diffraction patterns of powdered samples of HMP and LMP were obtained using a Philips PW1710 automated diffractometer, with monochromatized CuK_α ($K_{\alpha 1}$ = 1.54060 Å; $K_{\alpha 2}$ = 1.54438 Å) radiation. The diffractometer is equipped with a 2θ compensating

[1] Division of Pharmaceutics, College of Pharmacy, The University of Iowa, Iowa City, Iowa 52242.
[2] Current address: Pharmaceutical Products Division, D-493, R1B, Abbott Laboratories, North Chicago, Illinois 60064.
[3] To whom correspondence should be addressed.

0724-8741/93/1000-1507$07.00/0

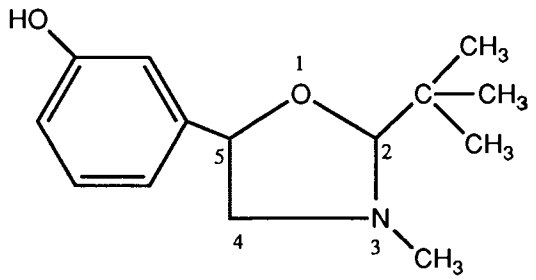

Fig. 1. Chemical structure of phenylephrine oxazolidine.

slit and a graphite monochomator. It was calibrated to within 0.02° (2θ) using the quartz peak at 26.66° (2θ). Patterns were scanned from 2 to 62° (2θ) at a scanning speed of 6°/min.

Solubility Measurements. The solubilities of HMP and LMP were determined in silicone fluid at two different temperatures. For testing at room temperature (~22°C) the solutions were placed in Teflon-lined, screw-capped glass test tubes and rotated end over end at 25 rpm for 24 hr. For testing at 37°C the solutions were placed in Teflon-lined, screw-capped glass vials and mechanically shaken in a thermostatically maintained water bath at a fixed rate of 196 strokes/min for 24 hr. After equilibration, the samples were filtered using 0.22-μm filter units (Millipore Corp., Bedford, MA) pretreated with silicone fluid and then analyzed for the prodrug content using a normal-phase HPLC assay.

Intrinsic Dissolution Testing. A nondisintegrating tablet of either HMP or LMP was prepared by the direct compression method from 400 mg of the crystals with a Carver press (Pasadena Hydraulics, Inc., El Monte, CA) under a pressure of 3000 lb for 4 min using a 13-mm-diameter punch and die set. The intrinsic dissolution rate was determined under the following conditions: medium, pH 7.4 isotonic phosphate buffer containing 0.01% ethylenediaminetetraacetic acid (EDTA); volume, 400 mL; temperature, 37 ± 1°C; stirring speed, 60 rpm; sampling volume, 2.0 mL; and sampling interval, 5, 10, 15, 20, 25, 30, 40, and 50 min. PO in the sample is rapidly converted ($t_{1/2}$ ≈10 min) to PE, and after at least nine half-lives elapsed, the samples were assayed for PE using a reversed-phase HPLC method.

X-Ray Crystallography. Single crystals of HMP were grown from acetone-petroleum ether by the slow evaporation method. A single crystal of LMP was selected from the bulk LMP using a microscope at low power.

For structure resolution, an HMP crystal measuring 0.15 × 0.40 × 0.50 mm was placed on a four-circle computer-controlled X-ray diffractometer (Model CAD 4, Enraf-Nonius, Bohemia, NY) equipped with a graphite crystal as an incident beam monochromator. Intensity data were collected using monochromated MoK_α radiation (0.7107 Å) at scan speeds of 1.5–5.0 deg/min, a scan range of 0.8 + tan(θ), a scan ratio (Ω/θ) of 1, and a theta range of 2–27.5 deg. The diffractometer was operated at 22°C. A least-squares refinement of 25 θ values (20° < 2θ < 28°) gave cell dimensions of a = 20.697 Å, b = 7.065 Å, and c = 9.304 Å. For a total of 3764 reflections measured (h, −24 to 26; k, 0 to 9; l, −12 to 12), only 1046 were unique and not systematically absent. The intensities were corrected for Lorentz and polarization factors, but not for absorption.

The data were merged using the SDP program to give 1800 unique reflections, merging R_{int} = 0.039, of which 1046 with $F > 2\sigma_F$ were used for the structural analysis. The structure was solved by direct methods, applying the Multan 80 program. An E-map calculated from the set of the phases with the highest figure of merit revealed the positions of all non-hydrogen atoms. Full-matrix least-squares techniques with anisotropic thermal parameters for nonhydrogen atoms were used to refine the structure. A difference Fourier map then revealed the position of all the hydrogen atoms and the hydroxyl group. The final refinement was then performed with the hydrogen atoms at theoretical positions (C−H = 0.95Å, −OH H atom from difference map) with a temperature factor of $B = 1.1\,B_{iso}$ of C atom, and reducing R to 0.052 and R_w to 0.068. The weighting scheme was $w = [\sigma_F^2 + (P^*F)^2 + Q]^{-1}$. The maximum shift/ESD is 0.05 for the last cycle. The final difference density map shows maximum electron density of 0.24 eÅ^{-3}.

Transformation. A sample of HMP crystals was heated dry in an oven at 68°C for 15 hr. LMP was heated at 70°C for 24 and 48 hr. A sample of either HMP or LMP was ground dry in a clean agate mortar with a pestle at room temperature for 5 min. A quantity of 400 mg of HMP or LMP was directly compressed into a tablet under two sets of conditions: a pressure of 5000 lb for 1.5 min and a pressure of 15,000 lb for 2.0 min, respectively. The surface layer of the tablet was gently removed with a spatula for examination. All samples were analyzed by DSC for transformation following thermal and mechanical treatment. After storage for 3 days, crystals of both HMP and LMP were collected from silicone fluid suspension samples stored at room temperature by vacuum filtration and analyzed by DSC.

Stereochemical Composition Analysis

Polarimetric Determination. The optical rotations of both HMP and LMP were determined using a digital polarimeter (Model DIP-360, Jasco, Inc., Easton, MD) under a set of standard conditions: cell length, 1 dm; wavelength, sodium doublet (589.0/589.6 nm); and temperature, 20°C. Acetone was used as the solvent. The concentrations of HMP and LMP were determined by HPLC assay.

NMR Spectroscopy. HMP or LMP was dissolved in deuterated acetone containing 1.0% TMS as a reference substance. The concentration of the sample was approximately 0.2 molar. The ^1H, homonuclear decoupling, nuclear Overhauser effect, and ^{13}C spectra were obtained at room temperature using an NMR spectrometer (Model WM360, Bruker Instrument Co., Billerica, MA).

Single-Crystal X-Ray Crystallography. The above-mentioned single-crystal X-ray diffraction study was also used for determination of molecular configurations of HMP and LMP.

RESULTS AND DISCUSSION

Crystal Morphology of HMP and LMP

The crystalline habits of HMP and LMP can clearly be distinguished in scanning electron microphotographs of the crystals (5). Crystals of HMP are lamellar with smooth faces, whereas LMP appears as tabular crystals with relatively rough surfaces over which there are some overgrowths. It

was observed that both crystal size and size distribution were similar for HMP and LMP. Crystals range in size from approximately 10 to 100 μm, with a slightly narrower size distribution for LMP.

Thermal Analysis

Thermal Microscopy. The sample identified as the HMP consisted mostly of birefringent variegated crystals. Melting began at 110.1°C and was complete by 112.5°C. The sample identified as the LMP consisted of nondescript clumps of particles, which appeared not to be birefringent, as well as crystals of various sizes and shapes, mostly parallelograms, which were birefringent. No thermal events were observed up to 106.8°C, where the first melting was observed. Melting was complete at 109.1°C.

DSC Results. Typical DSC thermograms of HMP and LMP recorded in the temperature range 90–115°C at a heating range of 1.0°C/min are presented in Fig. 2. Both materials exhibit a single endotherm corresponding to fusion. Three such measurements of HMP or LMP yielded the following data: ΔH_f = 131.32 ± 0.88 J/g, T_f = 109.52 ± 0.06°C, purity = 99.59 ± 0.04% for HMP; ΔH_f = 134.07 ± 1.66 J/g, T_f = 105.58 ± 0.03°C, purity = 99.22 ± 0.05% for LMP. The purities of the samples were determined by melting point depression based on van't Hoff's equation.

Quantitation of the Binary Mixture of HMP and LMP. In order to use the DSC technique as an analytical tool for quantitation of binary mixtures of HMP and LMP, a linear calibration curve was constructed between the percentage weight of HMP in the mixture (W_h%) and the percentage area of HMP (*A*%) obtained from the DSC scan based on the results of the prepared physical mixtures (5). The equation for the conversion of percentage area to the actual percentage of HMP in the sample was of the form:

$$A\% = 1.145\,(W_h\%) - 14.18, \qquad r = 0.9985$$

Infrared Spectra

Infrared spectra obtained using diffuse reflectance spectroscopy are similar for HMP and LMP (5). Only slight differences could be detected. The three most characteristic peaks are seen at 709, 867, and 1118 cm^{-1}. In both spectra, there is a peak at approximately 700 cm^{-1}, however, in the high-melting form this peak is a doublet, while it is a triplet in the low-melting form.

Powder X-Ray Diffraction Analysis

The powder patterns of HMP and LMP are given in Figs. 3 and 4, respectively. At every angle of diffraction the X-ray patterns are essentially superimposable except for different relative intensities of the peaks at a few angles. Powder patterns were also obtained on an instrument capable of higher resolution and were compared with the single crystal data (5). An excellent fit for the refinement was demonstrated in the final difference-profile plots.

Solubility and Intrinsic Dissolution Studies

Solubility in Silicone Fluid. Solubility was determined in order to compare the properties of HMP and LMP and to observe the effect of the dissolved drug in the silicone fluid on transformation in suspensions. The mean values of the solubility determinations were 0.416 mg/mL (n = 2) at 37°C and 0.248 mg/mL (SD = 0.0134; n = 4) at room temperature for HMP. The results of solubility testing for LMP were 0.516 mg/mL (n = 2) at 37°C and 0.261 mg/mL (SD = 0.0067, n = 4) at room temperature (~22°C). The solid samples were analyzed by DSC following equilibration. No transformation was observed after 36 hr, however, after 3 days partial transformation of LMP to HMP occurred.

Intrinsic Dissolution Rates. Dissolution from nondisintegrating tablets under fixed hydrodynamic conditions allows

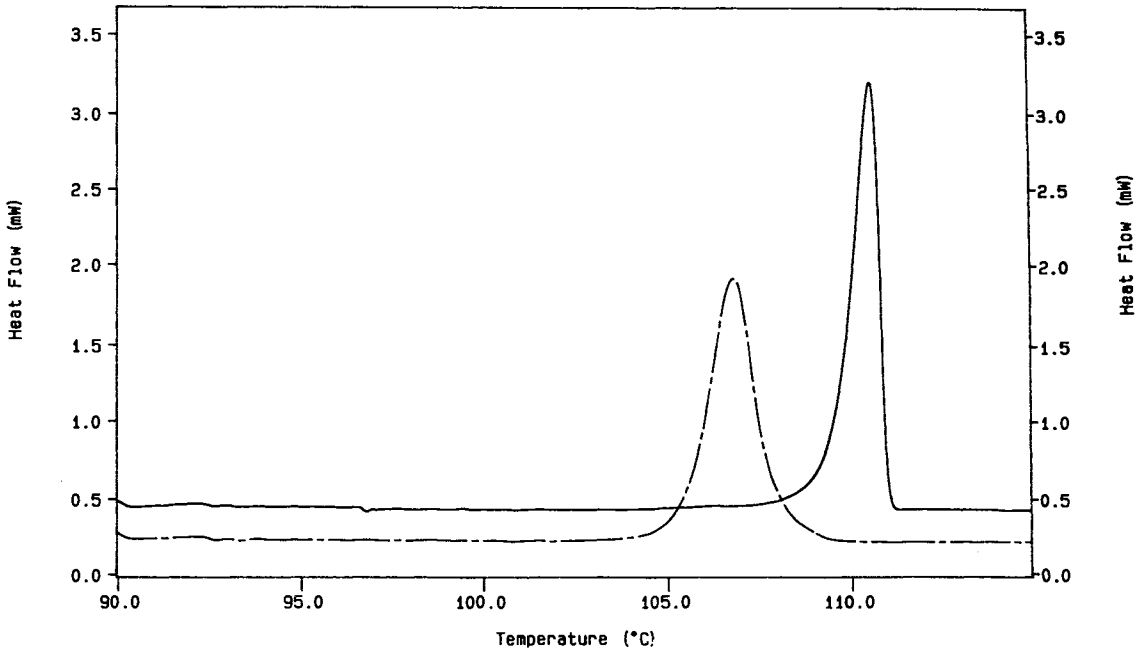

Fig. 2. Typical DSC thermograms of high-melting (solid line) and high-melting (dashed line) phenylephrine oxazolidine.

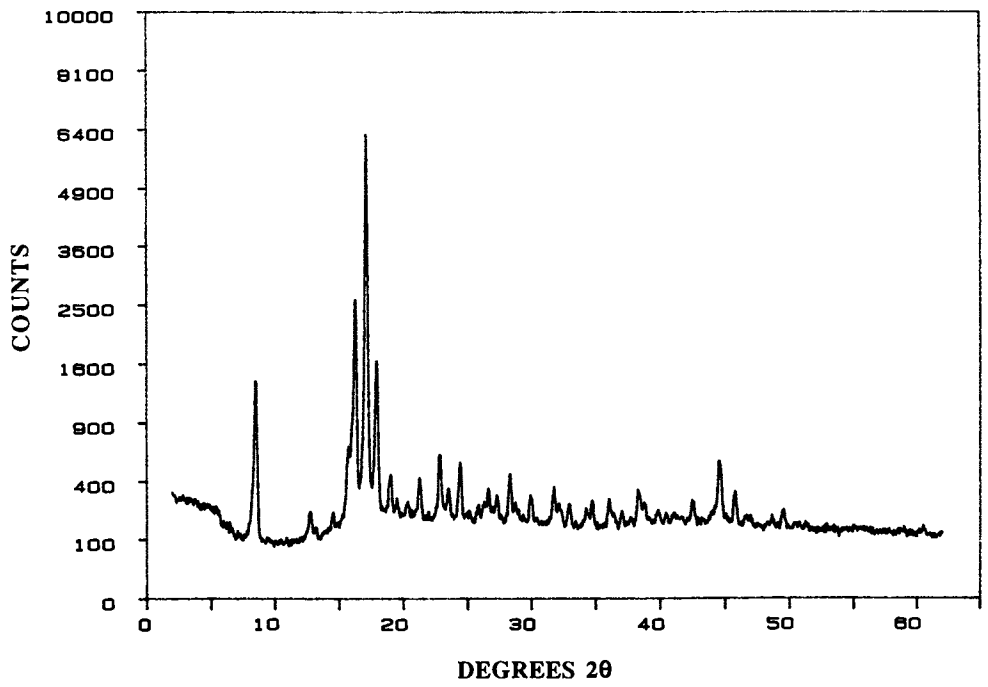

Fig. 3. X-ray powder pattern for HMP.

one to differentiate intrinsic dissolution properties of particular crystal states from effects of particle size, wetting, and other formulation related effects. For phenylephrine oxazolidine, the process of dissolution in water first involves solvation of the drug at the solid/solution interface, followed by diffusion accompanied by chemical reaction occurring across the boundary layer into the bulk. Diffusion and first-order hydrolysis from the thin layer of saturated solution at the solid surface into the bulk liquid under sink conditions are expected to be identical for HMP and LMP. Consequently, the dissolution rate measured from a disk with constant surface area can be considered to be the intrinsic dissolution of the crystalline drug.

For a dissolving disk under sink conditions with a constant surface area, the dissolution process can be described by (6):

$$W = kC_s t$$

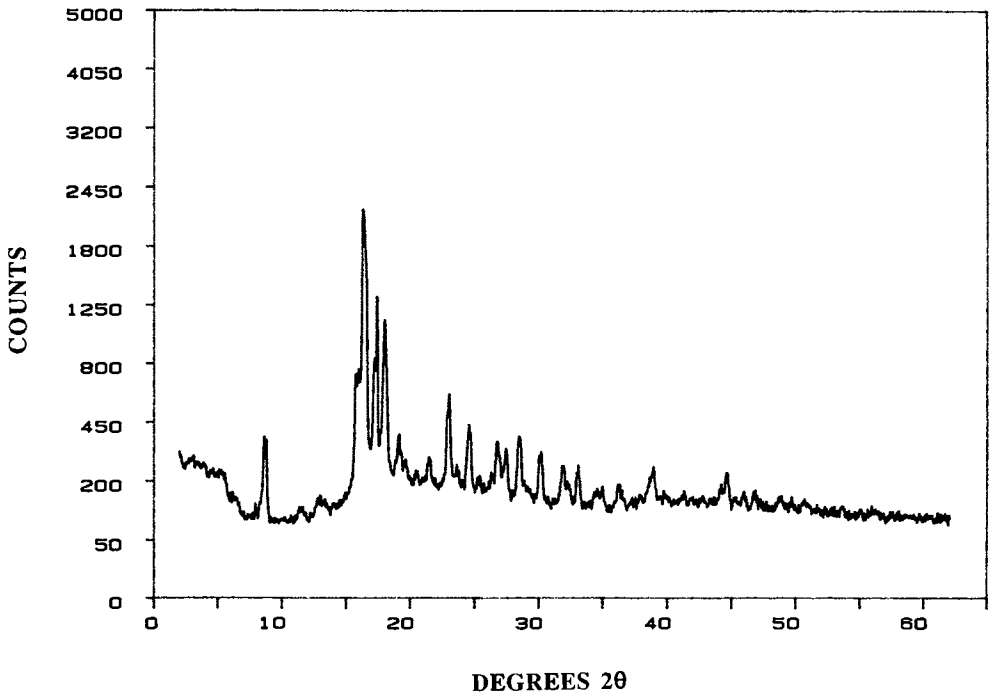

Fig. 4. X-ray powder pattern for LMP.

where W is the amount dissolved, C_s is the solubility of the compound, and k is a constant which includes the surface area of the dissolving disk, the diffusion coefficient, and the diffusion layer thickness. Thus, a plot of amount dissolved as a function of time should be linear for the initial dissolution, with the slope being equal to the intrinsic dissolution rate. The average intrinsic dissolution rates (5) were 0.048 ($\pm$0.0027) mg $\cdot$ cm^{-2} $\cdot$ min^{-1} for HMP and 0.074 ($\pm$0.0081) mg $\cdot$ cm^{-2} $\cdot$ min^{-1} for LMP. The dissolved amounts (mg) of the prodrug were calculated from the measured amounts of phenylephrine through molar conversion. It was found that the dissolution rate for LMP is 54.17% greater than that obtained for HMP (t = 9.795, $P < 0.005$).

Optical Activity

Two disastereomers of PO (5R/2S and 5R/2R) are expected to show different optical activity. However, optical purities as determined by optical rotation were found to be essentially the same for solutions prepared from HMP and LMP ([α] = $-105.8 \pm 0.85°$ for HMP vs [α] = $-102.2 \pm 3.90°$ for LMP; n = 4) and, therefore, do not provide sufficient evidence for the existence of two diastereomers.

NMR Studies

The assignments of protons in ^{1}H-HMR spectra of HMP and LMP were based on chemical shift values. The selected protons (δ = 2.85–4.85 ppm) were verified by a homonuclear decoupling experiment. Chemical shift nonequivalence of diastereotopic nuclei, as may be expected from a pair of diastereomers, was not observed in the two spectra. From a nuclear Overhauser effect (NOE) difference experiment involving irradiation of the C_2 t-butyl group, a small enhancement of H_5 in the trans diastereomer, but not the cis diastereomer was expected due to the through-space interaction between H_5 and protons in the t-butyl group. However no NOE enhancement was observed for either HMP or LMP solutions. Additional experiments also showed identical through-space interactions as determined by NOE.

Diastereomeric phenylephrine oxazolidines (5R/2R and 5R/2S) have diastereotopic t-butyl groups, $-C(CH_3)_3$, that are covalently linked in the molecule. They can be distinguished because the resonances of the diastereotopic nuclei are anisochronous and would normally be expected to give NMR signals with different chemical shifts in ^{13}C-NMR spectra. However, the NMR spectra of ^{13}C-NMR of HMP and LMP solutions were superimposable in all respects consistent with the formation of a single stereoisomer.

In summary, both ^{1}H- and ^{13}C-NMR results suggest that the HMP and LMP have the same stereochemical composition when determined in deuterated acetone.

Crystal and Molecular Structure

The single crystals of HMP and LMP selected for single-crystal analysis were identified by using DSC analysis. The molecular configuration, conformation, and the atom-numbering scheme of phenylephrine oxazolidine in the crystal of HMP and LMP are shown in Fig. 5. Selected bond angles are listed in Table I.

Molecular Geometry. The absolute configuration at the two asymmetric centers (C_2 and C_5) is 5R/2R where the C_2-t-butyl group in the isomer of the 1,3-oxazolidine formed from phenylephrine and pivalaldehyde is in the cis position relative to the C_5-phenyl group. N-methyl is in the trans position with respect to the C_2-t-butyl group. This is a result of the so-called nitrogen inversion in which the stereochemistry of the methyl may be inverted about the nitrogen atom depending on the temperature (7). In the determination of the inversion NMR is normally the method of choice. From the temperature dependence of the NMR spectra of 1,2,2-trimethylaziridine and N-methylpyrrolidine, the barriers to

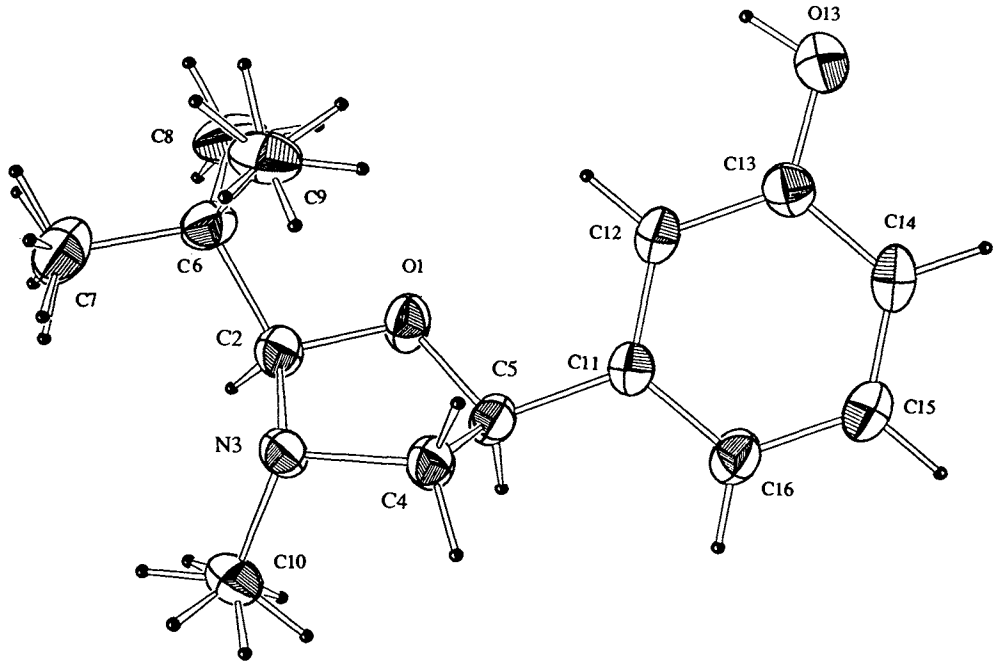

Fig. 5. Structure of the phenylephrine oxazolidine molecule in crystals of HMP and LMP.

Table I. Selected Bond Angles for High-Melting (HMP) and Low-Melting (LMP) Phenylephrine Oxazolidine[a]

Bond	Bond angle (°)	
	HMP	LMP
N3-C2-C6	115.2 (0.4)	117.0 (1.0)
O1-C2-C6	109.6 (0.3)	109.0 (1.7)
C4-C5-C11	114.0 (0.3)	116.3 (1.1)
O1-C5-C11	111.6 (0.3)	112.8 (1.1)
C2-N3-C10	110.9 (0.4)	111.0 (1.1)
C4-N3-C10	110.6 (0.3)	113.6 (11)

[a] Numbers in parentheses are estimated standard deviation. LMP data are obtained using fast data collection.

inversion have been calculated to be 20 and 7 kcal/mol, respectively. However, for phenylephrine oxazolidine, this dependency was not observed in the temperature range of 35 to −50°C due to the steric constraint caused by the C_2-t-butyl group. The plane through the C_5-phenyl ring is nearly perpendicular to the plane through the oxazolidine ring system. (The torsion angle C4-C5-C11-C12 is 95.04°.) Hydrogen atoms on *N*-methyl and two of the methyl groups in the t-butyl functionality are disordered and have two conformations of equal occupancy.

Crystal Packing and Hydrogen Bonding. Single crystal X-ray data are listed in Table II. Crystals of both HMP and LMP belong to the $P2_12_12_1$ space group with four molecules in an orthorhombic unit cell with dimensions a = 20.697(5) Å, b = 7.065(1) Å, and c = 9.304(2) Å. Figure 6 shows a projection of the unit cell of HMP. The unit cell for LMP was identical.

It was found that O(13) is the oxygen atom in the structure which acts as an acceptor of the hydrogen bond. Molecules of phenylephrine oxazolidine in the crystal form an intermolecular hydrogen bond between N(3) and O(13). The N(3)–O(13) distance is 2.846Å and the N(3)–H(13)–O(13) angle is 150.1°.

Table II. Crystallographic Parameters for the High- and Low-Melting Phenylephrine Oxazolidine Crystals (HMP and LMP)

Parameter[a]	HMP, $C_{14}H_{21}O_2N$	LMP, $C_{14}H_{21}O_2N$
a (Å)	20.697	20.676
b (Å)	7.065	7.068
c (Å)	9.304	9.298
Z	4	4
ρ_{calc} (g/cm^3)	1.15	1.15
Space group	$P2_12_12_1$	$P2_12_12_1$
Volume (Å^3)	1360.4	1358.6
R	0.052	0.092
R_w	0.068	0.088

[a] a, b, and c are unit cell axial lengths; Z is the number of molecules in a unit cell; ρ is the density; R is the unweighted agreement factor; R_w is the weighted agreement factor.

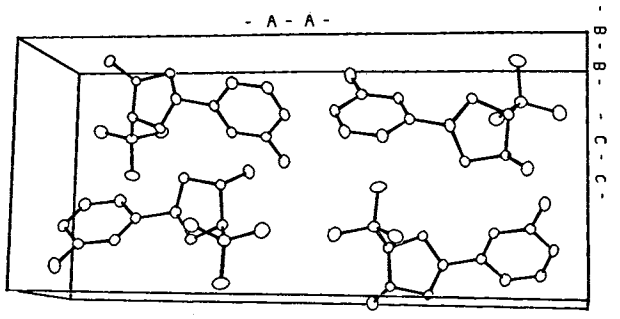

Fig. 6. Projection of the contents of the unit cell of HMP and LMP.

Both single-crystal X-ray and powder X-ray diffraction failed to detect any differences in lattice dimensions for HMP and LMP crystals, suggesting that there are no gross differences in crystalline structure between the two. Therefore, polymorphism is not a satisfactory explanation for the physical differences observed between HMP and LMP. Results from the FT-IR study also provide supplemental evidence for this conclusion.

Stereochemistry

All experimental evidence favors the conclusion that HMP and LMP are two crystal solids with identical stereochemical composition corresponding to a single molecular configuration of the cis diastereoisomer (5R/2R). On the basis of the mechanism of the condensation reaction of *l*-phenylephrine with pivalaldehyde (8), the synthesis is by no means an asymmetric reaction since there is neither chiral reagent nor steric hindrance present that may favor the stereospecific attack of the carbon by the paired electrons on the nitrogen atom during the formation of the oxazolidine ring. To determine the possible reasons for the isolation of a single isomer from the reaction solution, molecular energies were calculated for both *cis* and *trans* diastereomers using data from the X-ray structure and the program SYBYL operating on a Silicon Graphics (Mountain View, CA) workstation. The calculated potential energy function of the molecule includes stretching, bending, torsion, van der Waals, electrostatic interaction, and constraint terms. Gas-phase energies of each configuration were compared, and only minor differences were observed with a slightly higher energy for the cis isomer. Therefore, the preferential formation of the cis isomer following crystallization cannot be justified on the basis of an energy difference between the two stereoisomers.

The invocation of crystal forces to shift the equilibrium from one that is balanced in solution to an equilibrium that is essentially completely one-sided in the crystalline state requires further comment. There are numerous examples in the literature of instances in which the the great selectivity inherent in the crystallization process has been employed to obtain in pure form one or more isomeric species which are known to be in equilibrium in solution (also called crystallization-induced *asymmetric transformation*). These include crystallization of rotational conformers, equilibrium asymmetric transformers, *cis-trans* isomers, and diastereoisomeric hemiacetals, etc. (9). In many of the cases cited, it is

not clear whether the selectivity is due to a thermodynamic preference for one isomer in the crystalline state or due to preferential nucleation of one isomer. In the latter example the diastereomer equilibrium is continually displaced by crystallization of one of the two species until the totality of the diastereomer mass is present as a single pure diastereomer. While the first possibility corresponds to an *asymmetric equilibration* in solution, the second may be described as a *crystallization-induced asymmetric disequilibration* (10). The latter supposes that the rate of crystallization of the less soluble diastereomer is slower than the rate of equilibration of the two species in solution, two phenomena which, *a priori,* are unrelated to one another.

In the present study, the best explanation that is consistent with the preferential formation of a single diastereomer is that in which both diastereomers may be formed initially in the synthesis of the prodrug, and equilibrated in the reaction solution to give a mixture whose composition is unknown. However, recrystallization of the product mixture from the solution might allow the formation of the thermodynamically more favorable cis isomer (5R/2R).

Transformation

Effects of Thermal and Mechanical Treatment. Neither spontaneous solid-state transition during storage nor transformation between HMP and LMP occurred following heating, grinding, or compression as determined by DSC.

Effect of Medium. No change could be observed for samples of HMP in suspension in silicone fluid, while all crystals of LMP sampled underwent partial transformation to HMP, except for those stored for 4 months at low temperature (−16°C). The isothermal, solvent-mediated transformation in suspension is most likely a result of rearrangement of molecules in the crystal through selective dissolution and redeposition between crystals of different chemical potential. By this mechanism, the slightly higher solubility of LMP increases the probability for nucleation and growth of the more thermodynamically stable HMP. Thus, the less soluble HMP grows at the expense of the more soluble LMP during storage. (As LMP dissolves, the guest molecule is diluted.) The extent of transformation was significant following 3 days of storage at room temperature. The solubility of PO in silicone fluid at low temperature is less than that at high temperatures. The difference in solubility between HMP and LMP is also smaller, so there is a smaller nucleation probability and, thus, the transformation is retarded. These results suggest that to form a stable suspension, the less soluble HMP must be employed because it proves to be the form least susceptible to transformation and crystal growth.

A reviewer has suggested that the transformation from LMP to HMP does not occur as readily as low temperatures because the degree of supersaturation with respect to the more stable phase, HMP, is decreased. Alternatively, the solvent mediated transformation may be limited by the dissolution of the unstable phase, LMP. Thus, if the dissolution rate of LMP is significantly reduced with temperature, a slower transformation from LMP to HMP would be expected.

The Effect of Crystal Imperfections on Crystal Properties

A small proportion of an impurity or additive, which may be termed a "guest," can be present in atomic, ionic, or molecular form in solid solution or as a eutectic, creating impurity defects in the crystal lattice of the major component, the "host." Impurity defects may interact with, or give rise to, dislocations within the crystalline host. The bulk properties of the solid host are therefore altered by the presence of the guest. Molecules of the guest in the crystallization medium may be absorbed onto the surface of the host crystals and/or alter their crystal habit, while some dislocations emerge at the crystal surface. Thus the surface properties of the host may be changed by the presence of the guest. This causes significant modifications to the thermodynamic properties of both the bulk and the surface of the crystalline host and therefore affects pharmaceutically important properties (11,12). According to Grant, Chow, and co-workers (13–21), virtually all pharmaceutical solids contain impurities, which are often compounds introduced during the processes of synthesis, extraction, or even purification of the solid. These authors have shown that when trace amounts of structurally related additives are present during the crystallization of acetaminophen, adipic acid, or phenytoin, changes in crystal habit, surface features, size distribution, density distribution, specific surface area, crystal energy, and dissolution rate occur as a result of uptake of the additives by the growing crystals. These changes are attributed to the increased disorder introduced by the incorporation of additives in solid solution in the crystal lattice. Since the nature and concentration of impurities and imperfections often vary from one batch of crystals or powder to another, batch-to-batch or lot-to-lot variations may cause problems in formulation and processing, giving rise to lack of reproducibility and poor performance in the final product (1).

Most organic compounds crystallize to form ordered lattices whose structure is governed by directional intermolecular interactions, as a result of hydrogen bonding, or by the nature of molecular symmetry. In the most common case, the incorporated guest molecules undergo intermolecular interactions of a different type or possess symmetry properties, shape and size different from those of the host molecules. These alterations create more disorder in the host lattice than expected from simple mixing in the liquid since the crystalline state, being intrinsically more ordered than the liquid state, is more sensitive to the presence of guest molecules. Guest–host systems of this type will form only simple solid solutions due to the presence of the guest randomly distributed throughout the crystals over a limited range of composition (13).

In the present study, crystals modified by the presence of trace amounts of an unknown guest molecule in dispersion are thought to be responsible for the differences observed in crystal habit, thermal behavior, solubility, and intrinsic dissolution rate of HMP and LMP. Certain observations can be explained in terms of such crystal imperfections. For example, lot-to-lot variations of the ratio of LMP detected in synthetic phenylephrine oxazolidine raw materials have been found to range from 15 to 45%. This occurs as the extent of crystal imperfection varies with the concentration of the guest. Also, it was observed that the percentage LMP in the

recrystallized product was influenced more by the initial ratio of LMP than by the nature of the solvent, particularly in the case where rapid crystallization was used. When the starting percent LMP was low (<12%) and there was mother liquor remaining from slow recrystallization, pure HMP crystals were obtained in every solvent tested regardless of solvent polarity, because the concentration of the guest molecules was reduced below the level where inclusion occurred. In addition, somewhat more symmetrical peaks, as well as higher purities were observed in DSC thermograms of the higher melting form (99.59% purity and a sharper peak for HMP versus 99.22% purity and a slightly broader peak for LMP).

The factors most likely involved in the observed difference in the intrinsic dissolution rate include increased surface area created by crystal imperfections, crystal anisotropy such as the presence of crystal faces exhibiting different polarities, crystal defects at the surface and within the bulk of the crystals induced by the guest and/or by crystallization conditions, and the complex interplay of these factors. For an essentially surface reaction-controlled dissolution process, different faces of the crystals generally display different rates of dissolution, depending on their interactions with the solvent involved. In an aqueous solvent, the polar crystal faces tend to dissolve faster than the less polar faces. The overall dissolution rate can be expressed as a function of the relative contribution of individual faces possessing different polarities. For dissolution with constant surface area, the presence of the guest within the crystals may play an important role since the guest molecules incorporated into the crystal lattices can generate crystal defects or dislocations, which, being in high energy states, are the preferred sites of dissolution. Thus, the rapidity of the dissolution of a solid is governed by the availability of these sites. Finally a few unindexed lines in the powder X-ray pattern of LMP may correspond to the trace amounts of the guest molecules present in the crystals.

From the thermodynamic point of view, the formation of solid solutions can normally occur by substitution. For such molecular substitution to take place, the host and the guest molecules need to be structurally related and similar in size, shape, and therefore bonding strength. In the present case, the identification and further characterization of the guest molecule are the subject of further study. However it is reasonable at this point to speculate on some possible guest molecules with such properties. Since the concentration of the guest is normally less than 0.5% and LMP is always found in the synthesis product, it is conceivable that the guest may be introduced from the "pure" reactants, pivalaldehyde and *l*-phenylephrine, used for the synthesis. The two starting compounds are so dissimilar to the prodrug in structure that the possibility of either one of them being the guest can be dismissed. But other aldehydes which might be present as impurities in pivalaldehyde could potentially react with phenylephrine to form oxazolidine compounds and become guest molecules, since these products could be very similar to the prodrug in structure and in hydrogen bonding capability. Another potential guest might arise from condensation of pivalaldehyde with *d*-phenylephrine which might be present in *l*-phenylephrine as an optical impurity in trace amounts. If this were the case, it would explain the slightly weaker (102 vs 106°) optical rotation observed for LMP.

ACKNOWLEDGMENTS

The authors wish to thank the Angelini Pharmaceuticals, Inc., River Edge, NJ 07661, for their financial support, Dr. S. Alta Botha for the X-ray diffraction patterns and diffuse reflectance FT-IR spectra, Mr. Tom Moninger of the Electron Microscopy Facility, University of Iowa, for his assistance with the scanning electron photomicrographs, Dr. N. Baenziger and Dr. D. Swenson of the Department of Chemistry, University of Iowa, and Dr. V. Young, Iowa State University, for single crystal X-ray studies and helpful suggestions.

REFERENCES

1. D. S. Chien and R. D. Schoenwald. Improving the ocular absorption of phenylephrine. *Biopharm. Drug Disposit.* 7:453–462 (1986).
2. D. S. Chien and R. D. Schoenwald. Ocular pharmacokinetics and pharmacodynamics of phenylephrine and phenylephrine oxazolidine in rabbit eyes. *Pharm. Res.* 7:476–483 (1990).
3. R. D. Schoenwald, J. C. Folk, V. Kumar, and J. Piper. In vivo comparison of phenylephrine and phenylephrine oxazolidine instilled to the monkey eye. *J. Ocul. Pharmacol.* 3:333–340 (1987).
4. M. Miller-Meeks, T. A. Farrell, P. Munden, J. C. Folk, C. Rao, and R. D. Schoenwald. Phenylephrine prodrug: Report of clinical trials. *Ophthalmology* 48:222–226 (1991).
5. Q.-H. Qiu. *Physicochemical Characterization and Ocular Bioavailability of High and Low Melting Phenylephrine Oxazolidines*, Ph.D. thesis, University of Iowa, Iowa City, 1992.
6. W. C. Stagner and J. K. Guillory. Physical characterization of solid iopanoic acid forms. *J. Pharm. Sci.* 68:1005–1009 (1975).
7. J. B. Lambert and W. L. Oliver Jr.. Nitrogen inversion without retarding factors. *J. Am. Chem. Soc.* 91:7774–7775 (1969).
8. J. March. *Advanced Organic Chemistry. Reactions, Mechanisms and Structure*, John Wiley & Sons, New York, 1985.
9. D. Y. Curtin and J. H. Engelmann. Intramolecular oxygen-nitrogen benzoyl migration of 6-aroyloxyphenanthridines. *J. Org. Chem.* 37:3439–3443 (1972).
10. J. Jacques, A. Collet, and S. H. Wilen. *Enantiomers, Racemates, and Resolutions*, John Wiley & Sons, New York, 1981.
11. H. M. Burt and A. G. Mitchell. Effect of habit modification on dissolution rate. *Int. J. Pharm.* 5:239–251 (1980).
12. H. M. Burt and A. G. Mitchell. Crystal defects and dissolution. *Int. J. Pharm.* 9:137–152 (1981).
13. P. York and D. J. W. Grant. A disruptive index for quantifying the solid state disorder induced by additives or impurities. I. Definition and evaluation from heat of fusion. *Int. J. Pharm.* 25:57–72 (1985).
14. A. H. L. Chow, P. K. K. Chow, Z. S. Wang, and D. J. W. Grant. Modification of acetaminophen crystals: Influence of growth in aqueous solutions containing p-acetoxyacetanilide on crystal properties. *Int. J. Pharm.* 24:239–258 (1985).
15. A. H. L. Chow and D. J. W. Grant. Modification of acetaminophen crystals. II. Influence of stirring rate during solution-phase growth on crystal properties in the presence and absence of p-acetoxyacetanilide. *Int. J. Pharm.* 41:29–39 (1988).
16. A. H. L. Chow and D. J. W. Grant. Modification of acetaminophen crystals. III. Influence of initial supersaturation during solution-phase growth on crystal properties in the presence and absence of p-acetoxyacetanilide. *Int. J. Pharm.* 42:123–133 (1988).
17. A. H. L. Chow and D. J. W. Grant. Influence of crystallization

conditions on the physical properties of acetaminophen crystals: Evaluation by multiple linear regression. *Int. J. Pharm.* 51:115–127 (1989).
18. A. H. L. Chow and D. J. W. Grant. Physical factors influencing the aqueous dissolution rate of acetaminophen crystals doped with p-acetoxyacetanilide: Evaluation by multiple linear regression. *Int. J. Pharm.* 51:129–135 (1989).
19. A. H. L. Chow and C. K. Hsia. Modification of phenytoin crystals: Influence of 3-acetoxymethyl-5,5-diphenylhydantoin on solution phase crystallization and related crystal properties. *Int. J. Pharm.* 75:219–230 (1991).
20. J. D. Gordon and A. H. L. Chow. Modification of phenytoin crystals. II. Influence of 3-propanoyloxymethyl-5,5-diphenylhydantoin on solution phase crystallization and related crystal properties. *Int. J. Pharm.* 79:171–181 (1992).
21. M. J. Pikal and D. J. W. Grant. A theoretical treatment of changes in energy and entropy of solids caused by additives or impurities in solid solution. *Int. J. Pharm.* 39:243–253 (1987).